Ocean Systems Engineering, *Vol. 6, No. 3 (2016) 245-264*
DOI: http://dx.doi.org/10.12989/ose.2016.6.3.245

Free surface effects on 2-D airfoils and 3-D wings moving over water

Sakir Bal*

Istanbul Technical University, Department of Naval Architecture and Marine Engineering, 34469 Maslak-Sariyer, Istanbul, Turkey

(Received March 15, 2016, Revised August 12, 2016, Accepted August 25, 2016)

Abstract. The iterative boundary element method (IBEM) developed originally before for cavitating two-dimensional (2-D) and three-dimensional (3-D) hydrofoils moving under free surface is modified and applied to the case of 2-D (two-dimensional) airfoils and 3-D (three-dimensional) wings over water. The calculation of the steady-state flow characteristics of an inviscid, incompressible fluid past 2-D airfoils and 3-D wings above free water surface is of practical importance for air-assisted marine vehicles such as some racing boats including catamarans with hydrofoils and WIG (Wing-In-Ground) effect crafts. In the present paper, the effects of free surface both on 2-D airfoils and 3-D wings moving steadily over free water surface are investigated in detail. The iterative numerical method (IBEM) based on the Green's theorem allows separating the airfoil or wing problems and the free surface problem. Both the 2-D airfoil surface (or 3-D wing surface) and the free surface are modeled with constant strength dipole and constant strength source panels. While the kinematic boundary condition is applied on the airfoil surface or on the wing surface, the linearized kinematic-dynamic combined condition is applied on the free surface. The source strengths on the free surface are expressed in terms of perturbation potential by applying the linearized free surface conditions. No radiation condition is enforced for downstream boundary in 2-D airfoil and 3-D wing cases and transverse boundaries in only 3-D wing case. The method is first applied to 2-D NACA0004 airfoil with angle of attack of four degrees to validate the method. The effects of height of 2-D airfoil from free surface and Froude number on lift and drag coefficients are investigated. The method is also applied to NACA0015 airfoil for another validation with experiments in case of ground effect. The lift coefficient with different clearance values are compared with those of experiments. The numerical method is then applied to NACA0012 airfoil with the angle of attack of five degrees and the effects of Froude number and clearance on the lift and drag coefficients are discussed. The method is lastly applied to a rectangular 3-D wing and the effects of Froude number on wing performance have been investigated. The numerical results for wing moving under free surface have also been compared with those of the same wing moving above free surface. It has been found that the free surface can affect the wing performance significantly.

Keywords: WIG (Wing-In-Ground); airfoil, wing; iterative boundary element method; free surface; wave drag; lift

1. Introduction

Marine vehicles with high speeds can utilize air wings. WIG (wing-in-ground) effect craft and

*Corresponding author, Professor, E-mail: sbal@itu.edu.tr

http://www.techno-press.org/?journal=ose&subpage=7 ISSN: 2093-6702 (Print), 2093-677X (Online)

some racing boats including catamarans with hydrofoils can take advantage of air lifting surfaces to support completely or partially the vehicle weight. In the present study, the performance of 2-D (two-dimensional) airfoils and 3-D (three-dimensional) wings moving with a constant speed above free water surface has been investigated by an Iterative Boundary Element Method (IBEM). The clearance (vertical distance) between the airfoil (or wing) and free water surface can affect significantly the airfoil (or wing) characteristics, such as; pressure distribution, lift, drag values as well as the wave deformations on the free water surface. The calculation of the steady-state flow characteristics of an inviscid, incompressible fluid past 2-D foils and 3-D wings moving above free water surface has therefore practical importance for air-assisted marine vehicles.

Recently, 2-D WIG problem in close proximity to a free surface has been studied in (Zong *et al*. 2012). According to this 2-D theory, WIG effect is significant when the clearance is small and the free surface can be represented by a rigid wall in the case of high velocity. A subsonic lifting surface theory for three-dimensional WIG effect crafts in the cases of both solid ground surface and free surface has been developed by (Liang and Zong 2011). They have found that when the clearance is small, WIG effect is significant. In (Liang et al. 2013), the problems of both two- and three-dimensional biplanes operating near a free surface were solved by extending the classical lifting theories. Extensive numerical results were presented to show the effect of clearance (height from free surface) and distance between two foils on the results (lift coefficient, drag coefficient etc.). The WIG problems in the cases of both 2-D and 3-D were also studied by (Barber 2007). It was found that for low Froude numbers (Fr < 1), the surface deformation is a small depression of the surface beneath the foil. As the Froude number is increased, a small change in the shape of the deformation is observed. At a Froude number of 14 the surface is not a depression, but rather a rise beneath the foil. It was mentioned that this result also followed the trends shown by (Grundy 1986). Jung *et al*. (2012) on the other hand studied the endplate effect on the performance of 3D wings operating over free water surface. They have found that the end plate can cause a decrease in induced drag. Amiri *et al.* (2016) have formulated numerically the accelerations of aerodynamically alleviated marine vehicles in the phases of both landing and take-off. The developed model by them has also been validated with the existing experimental data. They asserted that any reduction in total resistance in the phase of take-off will result in a decrease in get-away speed and take-off run of an aerodynamically alleviated marine vehicle. Matveev (2014) has described a coupled aero-hydrodynamic model for a ram wing moving above water in steady motion. The factors affecting the aerodynamic performance of a ram wing and associated water surface deformations have been presented and it has been shown that an extent of blockage of wing sides can drastically change the ram wing lifting performance. A comprehensive survey of reviewing research and development of WIG effect technology can be found in (Rozhdestvensky 2006).

On the other hand, various numerical methods have been developed to treat the flows (cavitating or non-cavitating) around hydrofoils moving under free surface or without the effect of free surface. Important studies by using the boundary element methods for the flow analysis of 2-D and 3-D cavitating or noncavitating hydrofoils and propellers can be found in (Fine and Kinnas 1993) and (Kinnas and Hsin 1992). Specifically, the Boundary Element Methods (BEMs) have also been found to be computationally efficient and robust tools for the inviscid analysis of cavitating or non-cavitating flows around arbitrary geometries (including ship type of bodies) both in two- and three-dimensions under free surface as given in (Lee *et al*. 1992) and (Guanghua 2013). For instance, Kelvin and Rankine types of singularities have modeled the flow around cavitating or non-cavitating hydrofoil under a free surface, in (Lee *et al*. 1992) and (Bal *et al.* 2001),

respectively. The linearized free surface condition was used in both methods. An IBEM (iterative boundary element method) for the solution of cavitating or non-cavitating hydrofoil moving under a free surface was described in detail in (Bal and Kinnas 2002). The integral equation obtained by applying Green's theorem on the surfaces of the problem was divided into two parts; the cavitating hydrofoil part and the free surface part. The cavitating hydrofoil influence on the free surface and vice versa was considered via their potential values. Details of the present low-order potential-based panel method can be found in (Kinnas and Fine 1993). One of the most important reviews of boundary element methods up to the late 1970s was given in (Cheng and Cheng 2005), as well. This iterative method was modified and extended to apply to the surface piercing bodies inside a numerical towing tank or without a numerical towing tank and extensive numerical results of the method have been presented in (Bal 2007), (Bal 2008) and (Bal 2011).

In the present paper, however, the numerical method originally developed for cavitating or non-cavitating hydrofoils moving under a free surface is modified and applied to 2-D airfoils and 3-D wings moving over water. In the method applied here, the integral equation based on Green's theorem is divided into two parts: (i) the airfoil part (or wing part), (ii) the free surface part. These two problems are solved separately, with the effects of one on the others being accounted for in an iterative manner. It can be said that these two separate problems communicate each other via their potential values. This method has two advantages: i-) Solutions of sub-problems are easier to handle and organize than the full problem in terms of numerical implementation, ii-) Each sub-problem requires less computation time and less memory than the solution of full-problem. The airfoil part (or wing part) as well as the free surface part are modeled with constant strength dipole and source panels. Source strengths on the free surface are proportional to the derivative of the perturbation potential with respect to the vertical axis. They are expressed by using the linearized free surface condition, in terms of the second derivative of the perturbation potential with respect to the horizontal axis as in (Dawson 1977). The corresponding second order derivative on the free surface is calculated via application a backward finite difference scheme (Bal and Kinnas 2002). In order to prevent upstream waves the first and second derivatives of the perturbation potential with respect to horizontal axis are enforced to be equal to zero. No radiation condition is enforced at the downstream boundary for 2-D airfoil problem and 3-D wing problem and at the transverse boundaries for only 3-D wing problem. The potential induced by airfoil (or wing) on the free surface and the potential induced by free surface on airfoil (or wing) surface are considered on the right hand sides of each corresponding integral equation.

The method is first applied to 2D NACA0004 foil geometry with the angle of attack of four degrees to validate the present numerical method with that given in (Zong *et al*. 2012). The method is also applied to NACA0015 airfoil for another validation with experiments in case of ground effect. The effects of vertical distance on lift coefficient have been investigated. The method is then applied to NACA0012 foil geometry with the angle of attack of five degrees. The effects of vertical height between foil and calm free surface on pressure distribution and lift and drag coefficients have been discussed in detail. The effects of Froude number and clearance on wave elevation have been also investigated. The effects of Froude number on the aerodynamic performance of 3-D wing have then been discussed. The aerodynamic results of the wing moving under free surface have also been compared with those of the same wing moving above free surface.

2. Mathematical model

2.1 2-D Airfoil problem

It is considered that an airfoil over a free surface is subjected to a uniform inflow, as shown in Fig. 1. The x-axis is positive in the direction of uniform inflow and the z-axis is positive upwards. The undisturbed free surface is located at z = 0 while the vertical distance between foil and free surface is h. It is assumed that the fluid is inviscid and incompressible and the flow field is irrotational. Despite the mathematical model (governing equation and boundary conditions) was explained in detail in (Bal and Kinnas 2002) and (Bal 2011), it is summarized below for the completeness of the paper.

The perturbation potential,ϕ(x,z) and the total potential,Φ(x,z) should satisfy the Laplace's equation in the fluid domain

$$\nabla^2\Phi = \nabla^2\phi = 0 \tag{1}$$

The following boundary conditions should also be satisfied by perturbation potential ϕ:

i) Kinematic boundary condition on foil surface: The flow should be tangent to the foil surface

$$\frac{\partial\phi}{\partial \mathrm{n}} = -\vec{\mathrm{U}}\cdot\vec{\mathrm{n}} \tag{2}$$

where $\vec{\mathrm{n}}$ is the unit normal vector to the airfoil surface directed into the fluid (air) domain.

ii) Kutta condition: The velocity at the trailing edge of the foil should be finite

$$\nabla\phi = \text{finite}; \quad \text{at the trailing edge} \tag{3}$$

If $\vec{\mathrm{t}}$ is a unit vector in the direction of the mean velocity, the velocity in the stream line direction must be continuous across the surface

$$\vec{\mathrm{V}}^{+}\cdot\vec{\mathrm{t}} = \vec{\mathrm{V}}^{-}\cdot\vec{\mathrm{t}} \tag{4}$$

Eq. (4) may be written in terms of total potential Φ

$$\frac{\partial\Phi^{+}}{\partial \mathrm{t}} = \frac{\partial\Phi^{-}}{\partial \mathrm{t}} \quad \Rightarrow \quad \frac{\partial}{\partial \mathrm{t}}\left(\Phi^{+}-\Phi^{-}\right) = 0 \tag{5}$$

which means that the jump of the potential across the wake remains constant in the stream-wise direction

$$\Phi^{+}-\Phi^{-} = \phi^{+}-\phi^{-} = \text{constant in t direction} \tag{6}$$

Eq. (6) can be shown to reduce Morinos' Kutta condition (Kinnas and Hsin 1992) and (Bal 2011)

$$\phi^{+}-\phi^{-} = \phi_T{}^{+}-\phi_T{}^{-} = \Delta\phi_{\mathrm{w}} \tag{7}$$

where ϕ_T^{+} and ϕ_T^{-} are the values of the potential at the upper and lower sides of the foil trailing edge, respectively.

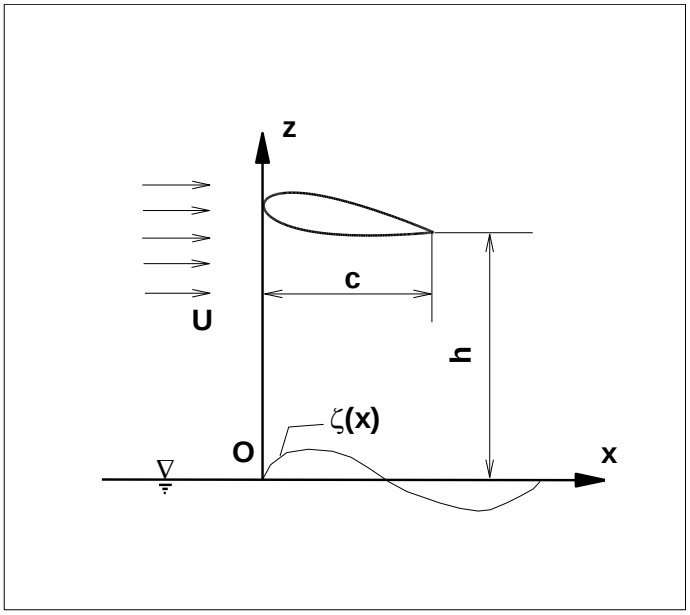

Fig. 1 Definition of coordinate system for 2D foil over water (not scaled)

iii) Kinematic free surface condition: The fluid particles should follow the free surface

$$\frac{DF(x,z)}{Dt} = 0 \quad \text{on } z = \zeta(x) \tag{8}$$

where $F(x,z)=z-\zeta(x)$.

iv) Dynamic free surface condition: The pressure on the free surface should be equal to the atmospheric pressure (p_{atm}). Applying Bernoulli's equation, the following equation can be given as,

$$\frac{1}{2}\left[(\nabla\Phi)^2 - U^2\right] + g\zeta = 0 \quad \text{on } z = \zeta(x) \tag{9}$$

where g is the gravitational acceleration. If the second-order terms are omitted and Eqs. (8) and (9) are combined, the following linearized free surface equation can be obtained as

$$\frac{\partial^2\phi}{\partial x^2} + k_0\frac{\partial\phi}{\partial z} = 0 \quad \text{on} \quad z = 0 \tag{10}$$

Here, $k_0=g/U^2$ is the wave number. The corresponding wave elevation in linearized form can also be obtained as

$$\zeta = -\frac{U}{g}\frac{\partial\phi}{\partial x} \tag{11}$$

v) Radiation condition: No upstream waves should occur. In order to prevent upstream waves, both the first-derivative and the second-derivative of the perturbation potential with respect to x is forced to be equal to zero for the upstream region on the free surface (Bal 2011)

$$\frac{\partial^2 \phi}{\partial x^2} = \frac{\partial \phi}{\partial x} = 0 \quad \text{as} \quad x \to -\infty \tag{12}$$

2.2 3-D Wing problem

It is considered similarly that the wing above free surface is subjected to a uniform inflow, U. The x-axis is positive in the direction of uniform inflow, the z-axis is positive upwards and the y-axis completes the right-handed system as shown in Fig. 2. The wing above undisturbed free surface is located at z = h. It is assumed that the fluid is inviscid and incompressible and the flow field is irrotational. The perturbation potential, $\phi(x,y,z)$ and the total potential, $\Phi(x,y,z)$ should satisfy the Laplace's equation in the fluid domain similar as in Eq. (1). The kinematic boundary condition, Eq. (2) and Kutta condition (including the boundary condition on the wake surface), as similar in Eq. (3), should also be satisfied by perturbation potential. An iterative pressure Kutta condition is forced at the trailing edge of the wing. The force-free condition is also satisfied on the wake surface. The trailing wake surface is assumed to be constant on z=h. The dipole strength in the wake however is convected along the assumed wake model in order to ensure that the pressure jump in the wake is equal to zero. In other words, in order for wake surface to be force-free, the pressure across the wake surface must be continuous

$$p^+ = p^- = p \qquad \text{on wake surface} \tag{13}$$

If $\vec{t}$ is a unit vector in the direction of the mean velocity, Eq. (13) implies that the streamwise velocity must be continuous across the surface

$$\vec{V}^+ \cdot \vec{t} = \vec{V}^- \cdot \vec{t} \tag{14}$$

Eq. (14) may be written in terms of Φ

$$\frac{\partial \Phi^+}{\partial t} = \frac{\partial \Phi^-}{\partial t} \quad \Rightarrow \quad \frac{\partial}{\partial t}\left(\Phi^+ - \Phi^-\right) = 0 \tag{15}$$

which means that the jump of the potential across the wake remains constant in the stream-wise direction

$$\Phi^+ - \Phi^- = \phi^+ - \phi^- = \text{constant in the t direction} \tag{16}$$

Eq. (16) can be shown to reduce iterative Morino's Kutta condition (Kinnas and Hsin 1992)

$$\phi^+ - \phi^- = \phi_T{}^+ - \phi_T{}^- = \Delta\phi_w \tag{17}$$

where $\phi_T{}^+$ and $\phi_T{}^-$ are the values of the potential at the upper and lower sides of the wing trailing edge, respectively. Refer to (Kinnas and Hsin 1992) for details.

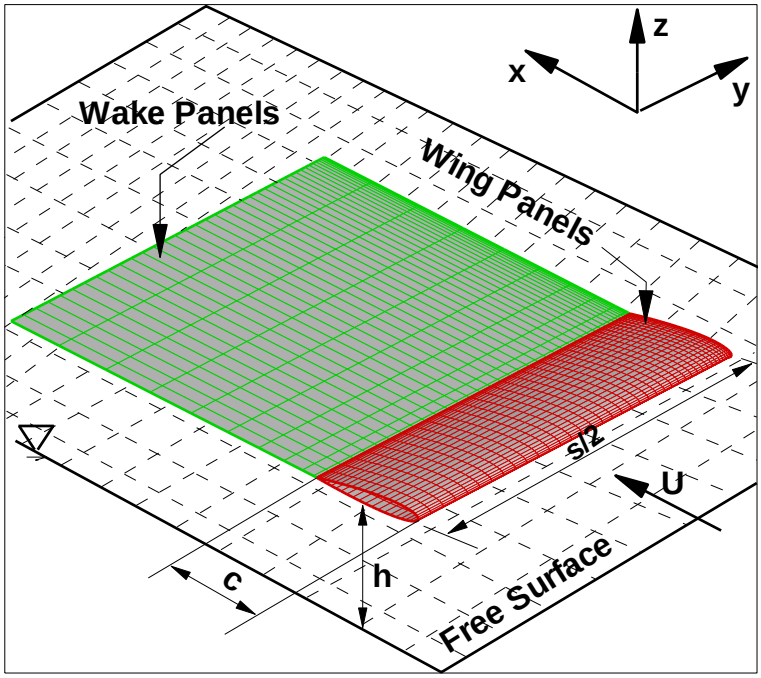

Fig. 2 Definition of coordinate system for 3-D wing problem. Half of the wing and its wake are shown due to symmetry (not scaled)

The linearized free surface condition which is identical to 2-D linearized condition as given in Eq. (10), should also be satisfied by perturbation potential ϕ(x,y,z). The related wave elevation in linearized form is identical to Eq. (11) as well. The radiation condition, on the other hand forces no upstream waves. It is also identical to that of 2-D problem as given in Eq. (12).

3. Iterative boundary element method

According to the Green's third identity the perturbation potential on the airfoil (or wing) surface and the free surface can be expressed as

$$C\pi\phi = \int_{S_F+S_{FS}} \left(\phi \frac{\partial G}{\partial n} - \frac{\partial \phi}{\partial n} G \right) dS + \int_{S_W} \Delta\phi_W \frac{\partial G}{\partial n^+} dS \tag{18}$$

where S_F, S_W and S_{FS} are the boundaries of the airfoil (or wing) surface, wake surface and the free surface, respectively. C is equal to 1 for 2-D airfoil problem and C=2 for 3-D wing problem. G is the Green function (G=ln r in 2-D airfoil problem and G=1/r in 3-D wing problem), (r is the distance between the singularity point and field point). $\Delta\phi_W$ is the potential jump across the wake surfaces, and n^+ is the unit vector normal to the wake surface pointing upwards. In the present study, the iterative method presented in (Bal 2011) is applied to solve Eq. (18). The iterative method here in general is composed of two parts: (1) the airfoil (or wing) part and (2) the free

surface part. On the other hand, the potential in the fluid domain due to the influence of the airfoil (or wing), ϕ_F, can be given as

$$C\pi\phi_F = \int_{S_F}\left(\phi\frac{\partial G}{\partial n} - \frac{\partial \phi}{\partial n}G\right)dS + \int_{S_W}\Delta\phi_W\frac{\partial G}{\partial n^+}dS \tag{19}$$

The potential in the fluid domain due to the influence of the free surface, ϕ_{FS} can be given as

$$C\pi\phi_{FS} = \int_{S_{FS}}\left(\phi\frac{\partial G}{\partial n} - \frac{\partial \phi}{\partial n}G\right)dS \tag{20}$$

By substituting Eq. (20) into Eq. (18), the following integral equation for the flow on the airfoil (or wing) surface can be written as

$$C\pi\phi = \int_{S_F}\left(\phi\frac{\partial G}{\partial n} - \frac{\partial \phi}{\partial n}G\right)dS + \int_{S_W}\Delta\phi_W\frac{\partial G}{\partial n^+}dS + 2C\pi\phi_{FS} \tag{21}$$

and by substituting Eq. (19) into Eq. (18) in a similar way the following integral equation for the flow on the free surface can be written as

$$C\pi\phi = \int_{S_{FS}}\left(\phi\frac{\partial G}{\partial n} - \frac{\partial \phi}{\partial n}G\right)dS + 2C\pi\phi_F \tag{22}$$

After applying the kinematic condition on the hydrofoil surface and linearized free surface condition, Eqs. (21) and (22) can be reduced to

$$C\pi\phi = \int_{S_F}\left(\phi\frac{\partial G}{\partial n} + Un_xG\right)dS + \int_{S_W}\Delta\phi_W\frac{\partial G}{\partial n^+}dS + 2C\pi\phi_{FS} \tag{23}$$

$$C\pi\phi = \int_{S_{FS}}\left(\phi\frac{\partial G}{\partial n} + \frac{\partial^2\phi}{\partial x^2}\frac{G}{k_0}\right)dS + 2C\pi\phi_F \tag{24}$$

Here, n_x is the x component of normal vector on the airfoil (or wing) surface. Integral Eqs. (23) and (24) can be solved iteratively by a low-order panel method with the potentials ϕ_F and ϕ_{FS} being updated during the iterative process. Here, the airfoil surface (or wing surface) and the free surface communicate each other via potential. The airfoil (or wing) surface and the free surface are discretized into panels with constant strength source and dipole distributions. The discretized integral equations provide two matrix equations with respect to the unknown potential values and can be solved by any matrix solver. In Eq. (24), the second derivative of perturbation potential term ($\partial^2\phi/\partial x^2$) can be expressed in terms of the potentials on the free surface by applying Dawson's original fourth-order backward finite difference scheme as given in (Bal and Kinnas 2002). In order to prevent upstream waves, the first derivative of potential with respect to x, ($\partial\phi/\partial x$) and the second derivative of potential with respect to x, ($\partial^2\phi/\partial x^2$) are enforced to be equal to zero. Thus the source strengths from some distance (termed *radiation distance*) in front of the airfoil (or wing) to

the upstream truncation boundary of the free surface are set to zero, and this forces the first derivative of potential with respect to z ($\partial\phi/\partial z$) to be equal to zero. The value of radiation distance is kept the same along the y axis in 3-D wing case. Details of the numerical method can be found in (Bal 2011).

4. Numerical results and discussion

The present boundary element method for the prediction of unbounded flow characteristics around surface piercing and fully submerged cavitating or non-cavitating hydrofoils has already been validated extensively in terms of convergence of the results and by comparison with experimental data and other numerical methods as given in (Bal 2008) and (Bal *et al.* 2001). The wave heights from present method for hydrofoil moving under free surface compared also satisfactorily with the experimental measurements as given in (Bal and Kinnas 2002). In addition, the results of the present numerical method for NACA0004 foil were compared with those of another numerical method for different angles of attack and Froude numbers (Zong *et al.* 2012).

4.1 NACA0004 Airfoil for Validation

The method is first applied to a NACA0004 airfoil with angle of attack of four degrees, $\alpha = 4^{\circ}$. The numbers of panels on the airfoil surface and on the free surface are chosen as, NF = 200 and NFS = 300, respectively. The clearance based Froude number is Fn_h=15. The ratios of vertical distances between airfoil and calm free water surface to chord are taken as h/c =1.5, 1.0, 0.6 and 0.4 and the corresponding chord based Froude numbers are Fn_c = 18.37, 15.00, 11.62 and 9.49, respectively, as given in (Zong *et al*. 2012). Here, the chord-based Froude number and clearance based Froude number are defined as $Fn_c = \frac{U}{\sqrt{gc}}$ and $Fn_h = \frac{U}{\sqrt{gh}}$, respectively. In Table 1, the calculated lift coefficients (C_L) are compared with those of given in (Zong *et al.* 2012).

The agreement between both results is satisfactory. This provides a strong validation test of the method. Note that for smaller h/c ratios, the lift coefficients become higher which is consistent with the results given in Zong *et al*. (2012) and Liang and Zong (2011) for very high Froude numbers.

Table 1 Comparison of lift coefficients with those of given in (Zong *et al*. 2012)

h/c	$Fn_h=U/(gh)^{0.5}$	$Fn_c=U/(gc)^{0.5}$	C_L (Values in Zong *et al*. 2012)	C_L (Values of Present Method)
1.5	15.00	18.37	0.53	0.53
1.0	15.00	15.00	0.55	0.55
0.6	15.00	11.62	0.60	0.61
0.4	15.00	9.49	0.66	0.67

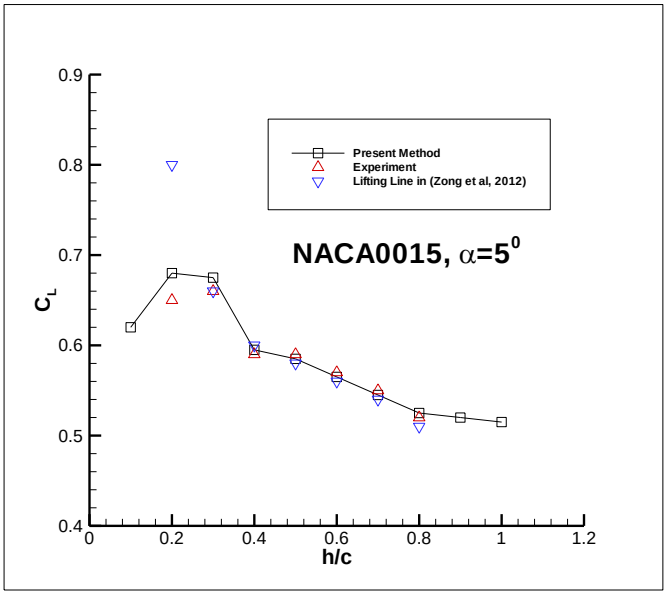

Fig. 3 Lift coefficient versus clearance-to-chord ratios in case of ground effect

4.2 NACA0015 airfoil for validation

The method is then applied to a NACA0015 airfoil with angle of attack of five degrees, $\alpha = 5^{\circ}$ in the case of ground effect for compariosn with experimental results . The numbers of panels on the airfoil surface and on the ground surface are chosen as, NF = 200 and NFS = 500, respectively. The ratios of vertical distances between airfoil and ground surface to chord are taken as between h/c =1.0, and 0.1, as given in (Zong *et al*. 2012). In Fig. 3, the calculated lift coefficients (C_L) are compared with those of experiments and a lifting line method given in (Zong *et al*. 2012). The agreement between pressent method and experiments is satisfactory even for small h/c ratios. This provides another strong validation test of the method. In Fig. 4, the corresponding pressure distributions are ahown for differnt h/c ratios. In this figure unbounded flow domain means no ground effect.

4.3 NACA0012 airfoil

The NACA0012 airfoil with $\alpha = 5^{\circ}$ is later chosen to present some extensive results. The Froude numbers are between $0.4 \leq Fn_c \leq 2.5$ and two clearance (vertical height between airfoil and calm free surface) to chord ratios are chosen as h/c = 1.0 and h/c=0.5. The numbers of panels on the airfoil surface and on the free surface are chosen as, NF = 300 and NFS = 500, respectively. the variation of lift and wave drag coefficients versus chord based Froude numbers with two different clearance/chord ratios (h/c=1.0 and h/c=0.6) is shown in Fig. 5. Note that the lift coefficients increased for increasing Froude numbers for both h/c ratios as a general trend. The lift coefficient in the unbounded flow domain (no free surface case) on the other hand is 0.58. The lift coefficient at Froude number $Fn_C = 2.5$ for h/c=1.0 is higher than the one in the unbounded flow domain. Note also that for Froude number $Fn_C = 1.5$, the wave drag coefficients decreased slightly for both h/c

ratios and then increased again for increasing Froude numbers. In Fig. 6, the effect of free surface on the pressure distribution on the airfoil has been shown for Fn_c=1.5 and h/c=1.0. Free surface has affected the pressure coefficient larger on lower surface than on the upper surface.

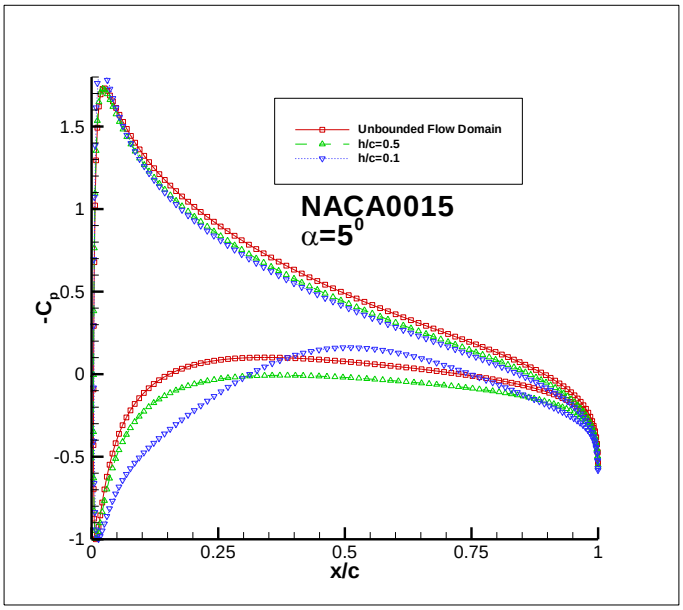

Fig. 4 Pressure distribution for different clearance-to-chord ratios in case of ground effect

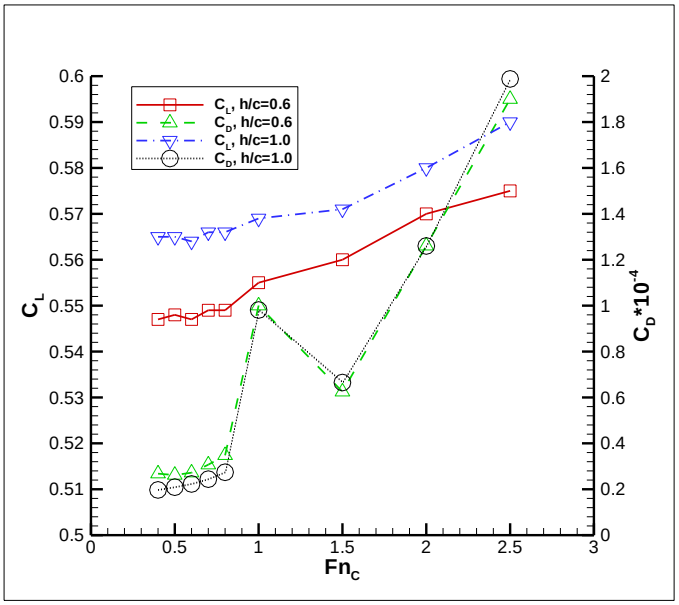

Fig. 5 Lift and drag coefficients versus Froude numbers with two different clearance-to-chord ratios

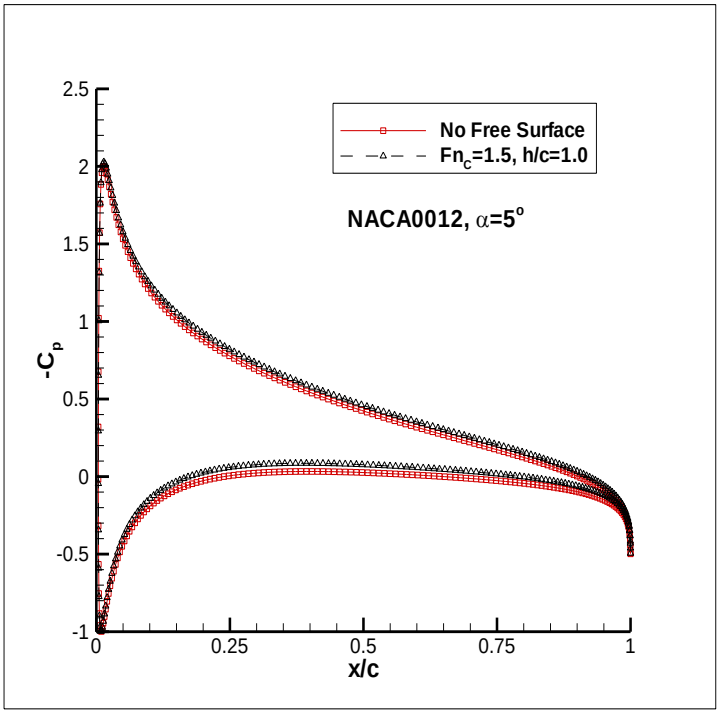

Fig. 6 Free surface effect on pressure distribution

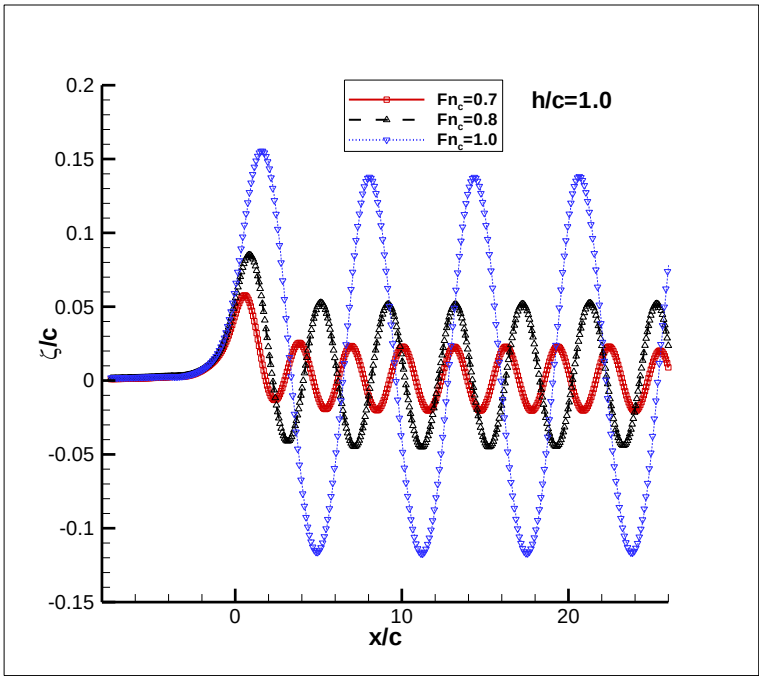

Fig. 7 Froude number effect on wave profiles for fixed clearance to chord ratio

In Fig. 7, the effect of Froude number on the wave deformation for fixed h/c = 1.0 has been presented. It has been found that increasing Froude numbers caused higher wave heights and larger wave lenghts. On the other hand, the smaller clearance-to-chord ratio (h/c) caused higher wave heights for fixed a Froude number as shown in Fig. 8. The clearance-to-chord ratios did not affect the wave lengths any more. In Fig. 9, the effect of iteration numbers on the lift and drag coefficients has been shown. Note also that the solution has practically converged within several iterations (here two) for both C_L and C_D.

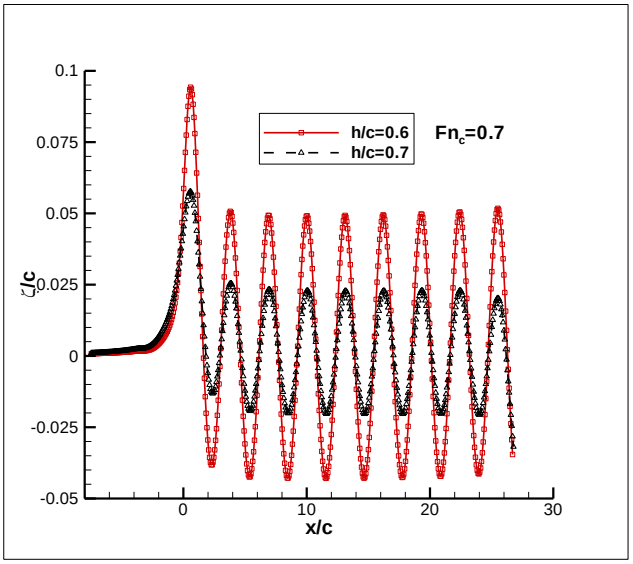

Fig. 8 Clearance-to chord ratio effect on wave profiles for fixed Froude number

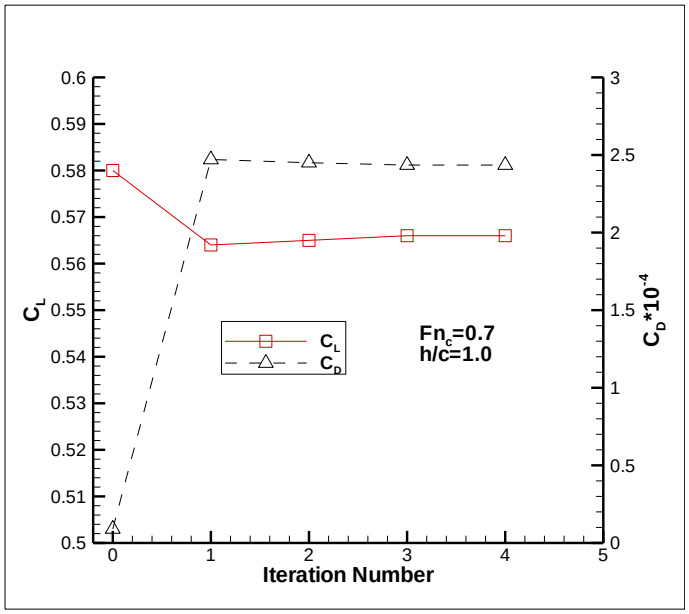

Fig. 9 Convergence history of the numerical method for lift and drag coefficients

4.4 3-D rectangular wing

The rectangular 3-D wing which has NACA0012 sections along span-wise direction has been modeled with AR (aspect ratio=s^2/A; A: planform area of wing) of 4. The chord length and span of the wing are represented as c and s, respectively, as shown in Fig. 2. The flow around the wing has been first simulated for the infinite case (no free surface effect, unbounded flow domain). The analyses have been performed for the angle of attack, α=5°. The total number of panels on the wing is 50x40=2000, (the number of panels along chord-wise direction and span-wise direction are 50 and 40, respectively) as shown half of the wing due to symmetry with respect to span in Fig. 2. On the other hand the total number of panels on the free surface is selected as 100x20=2000, (the number of panels along x direction and y direction are 100 and 20, respectively). The method applied here has also been validated before in the case of 3-D hydrofoils moving under free surface, including infinite case in (Bal 2008). So they are not repeated here. In Fig. 10, the non-dimensional pressure distribution ($C_P = \frac{p_0 - p}{\frac{1}{2}\rho U^2}$) for mid-strip, quarter-strip and tip-strip are given for the rectangular wing with AR=4 in unbounded flow domain. The variation of lift and drag (induced drag + wave drag) coefficients ($C_L = \frac{L}{\frac{1}{2}\rho A U^2}, C_D = \frac{D}{\frac{1}{2}\rho A U^2}$, L: lift force, D: drag force, A: planform area of the wing) with Froude number ($Fn = \frac{U}{\sqrt{gc}}$) is presented for two different h/c ratios (=0.5 and 1.0) in Fig. 11 The lift and drag coefficients (only induced) in the case of unbounded flow domain (no free surface effect) are computed as C_L=0.3283 and C_D=0.0095, respectively. Therefore for the selected range of Froude numbers the free surface caused an increase in both lift and drag coefficients. In Fig. 12, the wave contours on the free surface by IBEM are shown for Fn=0.7 and h/c=0.5. The Kelvin wave pattern can be seen clearly here. The pressure coefficients on the mid-section of the wing for Fn=0.7 and h/c=0.5 are shown as compared with those of infinite case in Fig. 13. Free surface caused an increase in pressure values which is consistent with the results given in Fig. 11.

Lastly the results of the 3-D wing moving under free surface have also been compared with those of the same wing moving above free surface. In Fig. 14, the non-dimensional pressure coefficients in the mid-strip for the wing moving under free surface (no cavitation model is included) are compared with those of the same wing with the same conditions (Fn=0.7 and h/c=1.0). The pressure coefficients in unbounded flow domain (no free surface effect) are also included in Fig. 14. Note that the pressure distribution on the lower side of the mid-strip has been increased slightly with respect to those of infinite fluid domain for the wing moving above free surface. On the other hand the pressure distribution on the upper side of the mid-strip has been increased slightly with respect to those of infinite fluid domain for the wing moving under free surface. Both are expected results. In Fig. 15, the wave contours on the free surface for the same wings with the same conditions are shown for both cases (above and under free surface). Note that the wave troughs created by the wing moving under free surface become wave crests created by the wing moving above free surface. The wave crests created by the wing moving under free surface become wave troughs created by the wing moving above free surface.

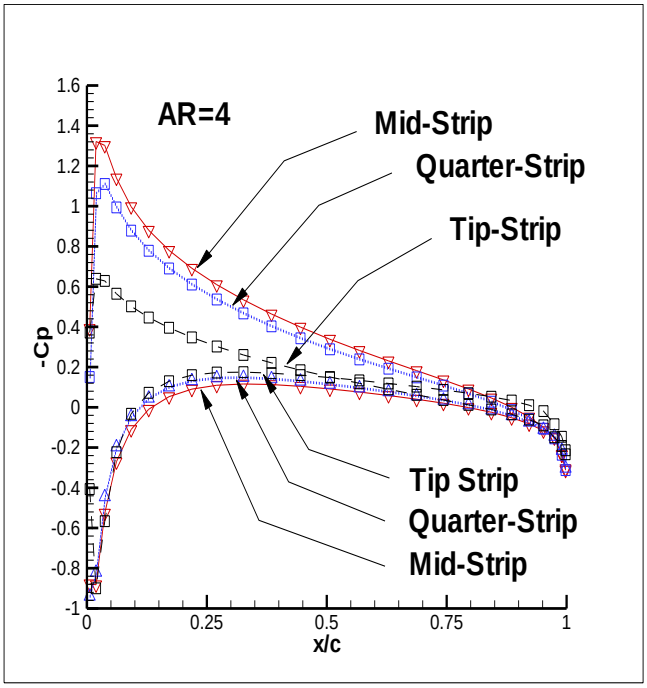

Fig. 10 Non-dimensional pressure distribution on rectangular wing with AR=4 in unbounded flow domain

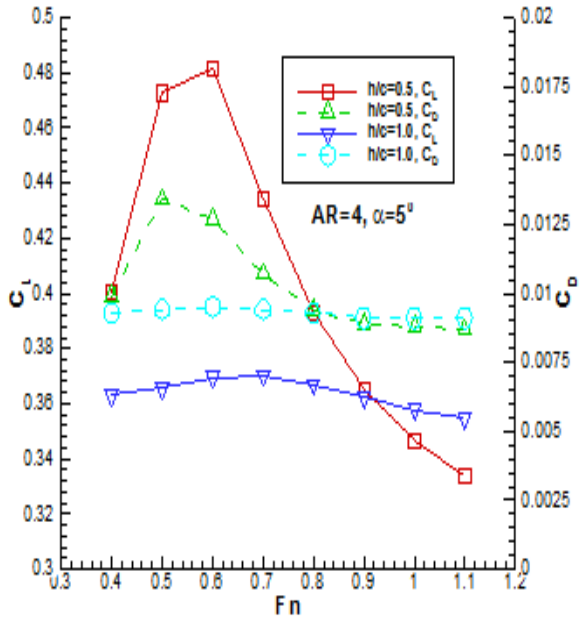

Fig. 11 Effect of Froude number on lift and drag coefficients for two different clearances

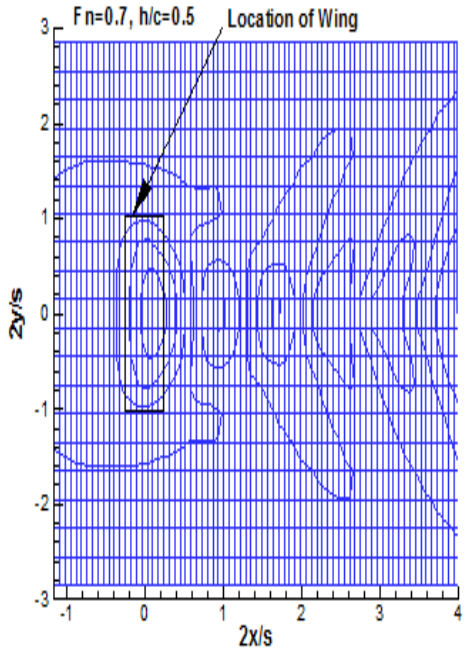

Fig. 12 Kelvin wave contours on free surface

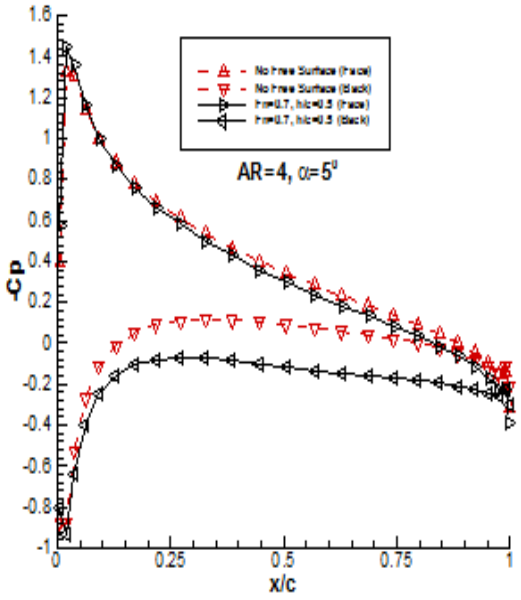

Fig. 13 Non-dimensional pressure distribution on mid-strip

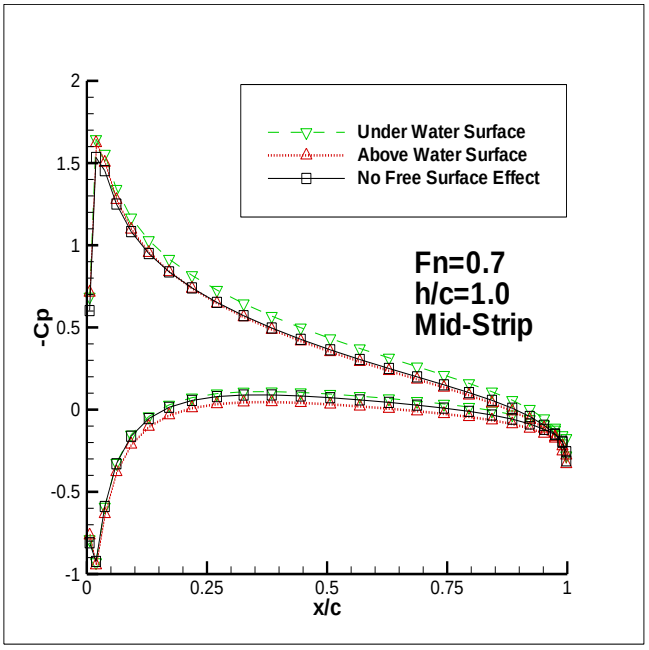

Fig. 14 Comparison of non-dimensional pressure coefficients in the mid-strip

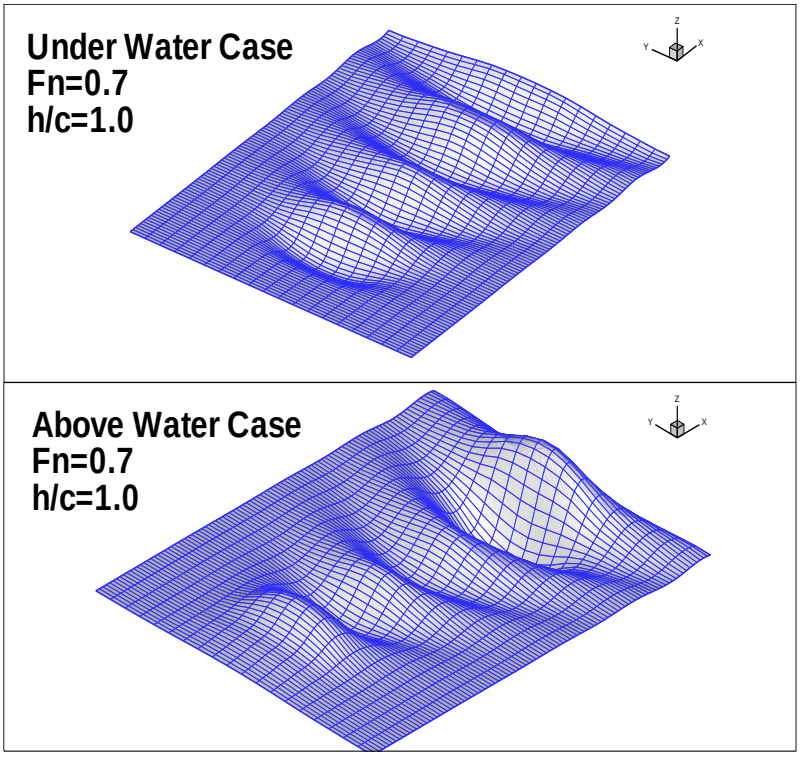

Fig. 15 Comparison of wave contours on the free surface

5. Conclusions

An iterative numerical method described for submerged cavitating hydrofoils under a free surface, has been modified and applied to 2-D airfoils and 3-D wings moving above free water surface and some numerical results have been presented. The iterative method was based on the perturbation potential formulation. The airfoil part (or wing part) and the free surface part were solved separately, with the effects of one on the other taken into account iteratively. These corresponding two problems communicate, or "talk" to, each other via their potential values. The iterative numerical method was first applied to NACA0004 airfoil geometry for validation. A satisfactory agreement has been found in terms of lift coefficient with different Froude numbers and clearance values. The method was then applied to NACA0015 airfoil for another validation with experiments in case of ground effect. A satisfactory agreement has also been found in terms of lift coefficient with different clearance values. The numerical method was later applied to NACA0012 foil with a constant angle of attack over a wider range of Froude numbers. It has been applied to a 3-D rectangular wing moving steadily over a free water surface to predict the aerodynamic performance. The followings have been found that:

1-) The loading on the 2-D airfoil is mainly increasing for increasing Froude numbers.
2-) The wave heights on the free surface is increasing for decreasing h/c ratios for a fixed Froude number for 2-D airfoil problem.
3-) The wave heights and wave lengths on the free surface are increasing for larger Froude numbers for a fixed h/c ratio both for 2-D airfoil problem and 3-D wing problem.
4-) The free surface caused an increase in loading (lift and drag coefficients and pressure distribution) of the 3-D wing related to those of infinite domain (the case of unbounded flow domain, no free surface effect).
5-) If the clearance is small, free surface effect on 3-D wing can become significant.
6-) The Kelvin wave pattern has also been occurred on the free water surface.
7-) The wave troughs created by the wing moving under free surface become wave crests by the wing moving above free surface and vice versa.
8-) It is also shown that the method is converged after several iteration steps.

It was also found that the effects of free surface on the performance of 2-D airfoils and 3-D wings can be substantial and should be considered in the design stage of the 2-D WIG sections and 3-D WIGs.

References

Amiri, M.M., Dakhrabadi, M.T. and Seif, M.S. (2016), "Formulation of a nonlinear mathematical model to simulate accelerations of an AAMV in take-off and landing phases", *Ships Offshore Struct*., **11**(2), 198-212.

Bal, S. (2008), "Performance prediction of surface piercing bodies in numerical towing tank", *Int. J. Offshore Polar Eng*., **18**(2), 106-111.

Bal, S. (2007), "High-speed submerged and surface piercing cavitating hydrofoils, including tandem case", *Ocean Eng*., **34**(14-15), 1935-1946.

Bal, S. (2011), "The effect of finite depth on 2-D and 3-D cavitating hydrofoils", *J. Marine Sci. Technol*., **16**(2), 129-142.

Bal, S. and Kinnas, S.A. (2002), "A Bem for the prediction of free surface effect on cavitating hydrofoils", *Comput. Mech*., **28**(3), 260-274.
Bal, S., Kinnas, S.A. and Lee, H. (2001), "Numerical analysis of 2-D and 3-D cavitating hydrofoils under a free surface", *J. Ship Res*., **45**(1), 34-49.
Barber, J.T. (2007), "A study of water surface deformation due to tip vortices of a wing-in-ground effect", *J. Ship Res.*, **51**(2), 182-186.
Cheng, A.H.D. and Cheng, D.T. (2005), "Heritage and early history of the boundary element method", *Eng. Anal. Bound. Elem*., **29**(3), 268-302.
Dawson, D.W. (1977), "A practical computer method for solving ship-wave problems", *Proceedings of the 2nd International Conference on Numerical Ship Hydrodynamics*, USA.
Fine, N.E. and Kinnas, S.A. (1993), "A boundary element method for the analysis of the flow around 3-D cavitating hydrofoils", *J. Ship Res.*, **37**(3), 213-224.
Grundy, I. (1986), "Airfoils moving in air close to a dynamic water surface", *J. Australian Math Soc. Series B*, **27**(3), 327-345.
Guanghua, H.E. (2013), "An iterative Rankine BEM for wave-making analyses of submerged and surface-piercing bodies in finite water depth", *J. Hydrodynamics*, **25**(6), 839-847.
Jung, J.H., Kim, M.J., Yoon, H.S., Hung, P.A., Chun, H.H. and Park, D.W. (2012), "Endplate effect on aerodynamic characteristics of three-dimensional wings in close free surface proximity", *Int. J. Naval Architect. Ocean Eng*., **4**(4), 477-487.
Kinnas, S.A. and Fine, N.E. (1993), "A numerical nonlinear analysis of the flow around two- and three-dimensional partially cavitating hydrofoils", *J. Fluid Mech*., **254**, 151-181.
Kinnas, S.A. and Hsin, C.Y. (1992), "A boundary element method for the analysis of the unsteady flow around extreme propeller geometries", *AIAA J*., **30**(3), 688-696.
Lee, C.S., Lew, C.W. and Kim, Y.G. (1992), "Analysis of a two-dimensional partially or supercavitating hydrofoil advancing under a free surface with a finite Froude number", *Proceedings of the 19th Symposium on Naval Hydrodynamics*, Korea.
Liang, H. and Zong, Z. (2011), "A subsonic lifting surface theory for wing-in-ground effect", *Acta Mech*., **219**(3), 203-217.
Liang, H., Zhou, L., Zong, Z. and Sun, L. (2013), "An analytical investigation of two-dimensional and three-dimensional biplanes operating in the vicinity of a free surface", *J. Marine Sci. Technol*., **18**(1), 12-31.
Matveev, K.I. (2013), "Modeling of finite-span ram wings moving above water of finite Froude numbers", *J. Ship Res*., **58**(3), 146-156.
Rozhdestvensky, K.V. (2006), "Wing-in-ground effect vehicles", *Progress in Aerospace Sciences*, **42**(3), 211-283.
Zong, Z., Liang, H. and Zhou, L. (2012), "Lifting line theory for wing-in ground effect in proximity to a free surface", *J. Eng. Mathematics*, **74**(1), 143-158.

MK

Nomenclature

AR : Aspect ratio
c : Chord length of airfoil or wing
C_D : Drag coefficient of airfoil or wing
C_L : Lift coefficient of airfoil or wing
C_P : Pressure coefficient
D : Drag of airfoil or wing
Fn_C : Chord based Froude number, $Fn_C = U/(gc)^{0.5}$
Fn_h : Clearance based Froude number, $Fn_h = U/(gh)^{0.5}$
g : Gravitational acceleration
h : Height between airfoil (or wing) and calm free surface
IBEM : Iterative boundary element method
k_0 : Wave number, $k_0 = g/U^2$
L : Lift of airfoil or wing
NF : Total number of panels on airfoil or wing surface
NFS : Number of panels on free surface
$\vec{n}$: Unit normal vector directed from airfoil (or wing) to air
p : Pressure
p_o : Reference pressure
s : Span of wing
S_{FS} : Free surface
S_F : Airfoil (or wing) surface
S_W : Wake surface
$\vec{t}$: Unit tangential vector on wake surface
U : Uniform velocity of incoming flow
α : Angle of attack
Φ : Total potential
ϕ : Perturbation potential
ρ : Density of water
ζ : Wave elevation